Microstructure and biopharmaceutical performances of curcumin-loaded low-energy nanoemulsions containing eucalyptol and pinene: terpenes' role overcome penetration enhancement effect?

Ines Nikolic , Evgenia Mitsou , Ivana Pantelic , Danijela Randjelovic , Bojan Markovic , Vassiliki Papadimitriou , Aristotelis Xenakis , Dominique Jasmin Lunter , Ana Žugic , Snezana Savic

PII: S0928-0987(19)30408-7
DOI: https://doi.org/10.1016/j.ejps.2019.105135
Reference: PHASCI 105135

To appear in: *European Journal of Pharmaceutical Sciences*

Received date: 18 June 2019
Revised date: 29 September 2019
Accepted date: 30 October 2019

Please cite this article as: Ines Nikolic , Evgenia Mitsou , Ivana Pantelic , Danijela Randjelovic , Bojan Markovic , Vassiliki Papadimitriou , Aristotelis Xenakis , Dominique Jasmin Lunter , Ana Žugic , Snezana Savic , Microstructure and biopharmaceutical performances of curcumin-loaded low-energy nanoemulsions containing eucalyptol and pinene: terpenes' role overcome penetration enhancement effect?, *European Journal of Pharmaceutical Sciences* (2019), doi: https://doi.org/10.1016/j.ejps.2019.105135

Microstructure and biopharmaceutical performances of curcumin-loaded low-energy nanoemulsions containing eucalyptol and pinene: terpenes' role overcome penetration enhancement effect?

Ines Nikolic[1], Evgenia Mitsou[2], Ivana Pantelic[1], Danijela Randjelovic[3], Bojan Markovic[4], Vassiliki Papadimitriou[2], Aristotelis Xenakis[2], Dominique Jasmin Lunter[5], Ana Žugic[6], Snezana Savic[1*]

[1]Department of Pharmaceutical Technology and Cosmetology, Faculty of Pharmacy, University of Belgrade, 11221 Belgrade, Serbia

[2]Institute of Chemical Biology, National Hellenic Research Foundation, 11635 Athens, Greece

[3]Institute of Chemistry, Technology and Metallurgy, Department of Microelectronic Technologies, University of Belgrade, 11000 Belgrade, Serbia

[4]Department of Pharmaceutical Chemistry, Faculty of Pharmacy, University of Belgrade, 11221 Belgrade, Serbia

[5]Institute of Pharmaceutical Technology, Eberhard-Karls University, D-72076 Tübingen, Germany

[6] Institute for Medicinal Plant Research "Dr Josif Pančić", 11000 Belgrade, Serbia

*Corresponding author:
Dr Snežana Savić,
Department of Pharmaceutical Technology and Cosmetology,
Faculty of Pharmacy, University of Belgrade,
Vojvode Stepe 450, 11221 Belgrade, Serbia

Tel.: +381-11-3951288; Fax: +381-11-3972840

E-mail address: snezana.savic@pharmacy.bg.ac.rs

Abstract

The objective of this work was to develop low-energy nanoemulsions for enhanced dermal delivery of curcumin, using monoterpene compounds eucalyptol (EUC) and pinene (PIN) as chemical penetration enhancers.

Spontaneous emulsification was the preparation method. All formulations contained 10% of the oil phase (medium-chain triglycerides (MCT), or their mixture with EUC or PIN. Formulations were stabilized by the combination of polysorbate 80 and soybean lecithin (*surfactant-to-oil-ratio*=1). Concentration of curcumin was set to 3 mg/ml.

Average droplet diameter of all tested formulations ranged from 102nm to 132nm, but the ones containing monoterpenes had significantly smaller size compared to the MCT formulation. Such finding was profoundly studied through electron paramagnetic resonance spectroscopy, which proved that the presence of monoterpenes modified the nanoemulsions' interfacial environment, resulting in droplet size reduction. The release study of curcumin (using *Franz* cells) demonstrated that the cumulative amount released after 6h of the experiment was 10.1±0.2% for the MCT nanoemulsions, 13.9±0.1% and 14.0±0.2% for PIN and EUC formulations, respectively. *In vivo* tape stripping revealed their performances in delivering curcumin into the skin, indicating the following order: EUC>MCT>PIN. The formulation with EUC was clearly the most successful, giving the highest cumulative amount of curcumin that penetrated per surface unit: 34.24±5.68 μg/cm^2. The MCT formulation followed (30.62±2.61 μg/cm^2) and, finally, the one with PIN (21.61±0.11 μg/cm^2). These results corelated with curcumin's solubility in the chosen oils: 4.18±0.02 mg/ml for EUC, 1.67±0.04 mg/ml for MCT and 0.21±0.01 mg/ml for PIN. Probably, higher solubility in the oil phase of the nanoemulsion promoted curcumin's solubility in the superficial skin layers, providing enhanced penetration.

Keywords:
Monoterpene; Low-energy nanoemulsion; Electron paramagnetic resonance spectroscopy; Interfacial dynamics; Penetration; Curcumin

1. INTRODUCTION

The concept of local treatment of some specific medical conditions using nanocarriers as drug delivery systems has gained more attention, aiming to enhance therapeutic effectivity and possibly reduce side-effects (Mishra *et al*, 2018; Krukiewicz and Zak, 2016). In this context, the skin offers a simple and convenient way for drug administration (Matos *et al*, 2019; Munch *et al*, 2018). However, transport of an active molecule into/through the skin still acts as a challenge, due to the specific cutaneous barrier. This barrier function is primarily ensured by the external layer – *stratum corneum*, a structure comprised of thickly packed keratinized cells (corneocytes), surrounded by a complex lipid-protein domain (Zsiko *et al*, 2019; Munch *et al*, 2017; Lane, 2013). In order to overcome it, several methods have been proposed. A novel approach is reflected in designing nanocarriers as drug delivery systems. Due to the small size of dispersed phase, higher drug loading capacity and potential for interactions with the superficial skin lipid and protein domains, nanocarriers can significantly contribute to drug penetration and availability (Un Din *et al*, 2017; Neubert, 2011; Mason *et al*, 2016).

In this context, among many possible nanoformulations, *oil-in-water* low-energy nanoemulsions, as prospective lipid-based nanocarriers, have drawn attention. These colloidal systems are characterized by high solubilization capacity for hydrophobic active molecules and ability to protect them from degradation. Moderate preparation conditions and inherent resistance to stability issues make them even more suitable as candidates for drug delivery systems (Komaiko and McClements, 2016). On the other hand, there is a long-standing approach of adding chemical penetration enhancers in the formulations, in order to alter *stratum corneum* cohesivity, causing higher fluidity and, consequently, enhanced drug molecule permeability (Neubert, 2011; Mohammed *et al*, 2014; Haque and Talukder, 2018)

It is expected that penetration enhancers can induce fluidization of the *stratum corneum* lipids and proteins or increase the partitioning of the active molecule into the *stratum corneum* (Lane, 2013). Among several classes of most common chemical penetration enhancers cited in the literature (including surfactants, alcohols and glycols, fatty acids and their esters…), terpenes have been established as effective penetration enhancers with lower skin irritation compared to conventional, synthetic ones (Pham *et al*, 2015; Ahad *et al*, 2009). They are volatile and fragrant compounds composed of isoprene units, found in essential oils (Zhu et al, 2019; Chen et al, 2016; Bilia et al, 2014; Dos Anjos, et al, 2007). Several terpenes (eucalyptol, menthol and menthone) are declared as *generally recognized as safe* (GRAS) by the US Food and Drug Administration. However, available bibliographical sources do not offer a satisfying level of information for terpene-governed penetration enhancement in humans (Lane, 2013). Penetration enhancement mediated by terpenes is generally accepted. However, this class of compounds is very heterogeneous. In order to elucidate the exact mechanism of the specific terpene responsible for the penetration of an active molecule, its physicochemical characteristics, interactions with other components of the formulation and with the skin should be profoundly studied (Yang et al, 2017; Karande and Mitragotri, 2009).

Based on the substantial research evidence, but also traditional use, curcumin, a polyphenol of natural origin, appeared opportune active molecule for treating various skin disorders (Ahangari *et al*, 2019; Choudhary *et al*, 2019; Panahy *et al*, 2019; Mohammad *et al*, 2018; Mouthuy *et al*, 2017, Vaughn *et al*, 2016; Thangapazham, 2007). Some of them, such as psoriasis, skin cancer or scleroderma require penetration of an active molecule in deeper skin layers for successful treatment (Thangapazham, 2007). However, highly demanding physicochemical characteristics of curcumin discourage its more intense concrete application (Panahi *et al*, 2019).

Therefore, the general goal of this work is to evaluate curcumin-loaded low energy nanoemulsions with terpene compounds (eucalyptol and pinene) in terms of their ability to enhance the penetration of curcumin through superficial skin layers *in vivo*, combining two strategies (nanotechnology and chemical penetration enhancers) for altering the cohesivity of *stratum corneum*. Special focus was put on a structural investigation in order to shade more light on the interactions of the formulation components that affect the performances of designed delivery system. In addition, the ability of these two terpene compounds to act as co-stabilizers in developed low-energy nanoemulsions was also assessed in a comprehensive manner, aiming to address their specific property to influence the interfacial phenomena, which has not been previously described in this manner. Data on curcumin stability and antioxidant efficacy after encapsulation were also provided.

Taken together, linking microstructural analysis and molecular interactions in the vehicle with biopharmaceutical performances offered a new perspective in elucidation of penetration enhancement efficacy in general.

2. MATERIALS AND METHODS

2.1.Materials

For sample preparation following chemicals were used: curcumin, pinene, eucalyptol (Sigma–Aldrich Co; St. Louis, USA), soybean lecithin S75 (Lipoid GmbH; Ludwigshafen, Germany), polysorbate 80 (Acros Organic, Thermo Fisher Scientific Company; Geel, Belgium), and medium-chain triglycerides (MCT, Miglyol 812, Fagron GmbH & KG; Barsbüttel, Germany). Ultrapure water was provided by the Gen Pure apparatus (TKA Wasseranfbereitungs system GmbH, Neiderelbert, Germany). For spin probing, 5-doxyl stearic acid was used (Sigma Aldrich, Germany). All other chemicals used in the experimental work were of pharmaceutical or HPLC grade and used as received, without further purification

2.2.Methods

2.2.1. Formulation preparation

Spontaneous emulsification method was used as a preparation technique. Each formulation contained 10% of the oil phase, and 10% of the surfactants (surfactant-to-oil ratio = 1). A mixture of oil and surfactants was prepared, and it was ~~being~~ added dropwise to the water phase, under constant magnetic stirring at 1000 rpm. After the whole amount of the blend had been used, systems were under constant stirring during the 1-hour period. The oil phase consisted of medium-chain triglycerides, or the combination of medium-chain triglycerides and terpene compound in the ratio 1:1. Based on previous research (Nikolic *et al*, 2018), polysorbate 80 and soybean lecithin in the ratio 9:1 were used as stabilizers. In case of curcumin-loaded formulations, the active molecule was firstly completely dissolved in the mixture of the oil phase and surfactants, and then added to the water phase as previously described. Curcumin was solubilized so that the final concentration in the nanoemulsions was 3 mg/ml, representing the

maximum solubilization capacity (Nikolic et al, 2018). After preparation, each nanoemulsion was packed in a crimped glass bottle and stored at 25 ˚C, protected from direct sunlight exposure.

2.2.2. Solubility study of curcumin in selected excipients

Solubility of curcumin in different excipients was evaluated through the shake flask method, utilizing orbital shaker IKA® KS 260 basic (IKA® Werke GmbH & Company KG Staufen, Germany). Details are given in the *Supplementary material* section.

2.2.3. Size analysis of dispersed oil droplets in low energy nanoemulsions

For size measurement, laser diffraction was performed, using Mastersizer 2000 (Malvern Instruments Ltd, Malvern, UK). The obscuration range was 2-6%. This technique provided volume weighted diameters d(10), d(50), d(90) and D[4,3] as relevant sizing parameters in the range 20nm - 2000µm.

2.2.4. Electrical conductivity and pH measurements

Electrical conductivity was measured using the Sensio +EC 71 conductivity meter (Hach Lange GmbH, Germany). Assessment of the pH values of the formulations was performed using HI2221 pH-meter (Hanna Instruments Inc, Michigan, USA).

2.2.5. Atomic force microscopy

To visualize dispersed nanodroplets of optimal low-energy nanoemulsions – to determine their morphological properties and to confirm data obtained on mean droplet size, atomic force microscopy was carried out applying AutoProbe CP-Research SPM (TM Microscopes-Bruker), using 90 µm large area scanner. Formulations were diluted with ultra-pure water (1:50 v/v), and 10 µL of diluted sample was placed on circular mica substrate (Highest Grade V1 AFM Mica Discs, Ted Pella Inc., Redding, California, USA) and dried in vacuum. Due to the nature of the

samples, noncontact mode was applied. AFM measurements were performed in air, using noncontact probes Bruker Phosphorous (n) doped silicon Tap300, model MPP-11123-10 with Al reflective coating and symmetric tip. Driving frequency of the cantilever was about 300 kHz. Both topography and "error signal" AFM images were taken and later analyzed.

2.2.6. Interfacial dynamics assessment Electron paramagnetic spin resonance spectroscopy

In order to evaluate the influence of terpene addition to dynamics of the water-oil interfacial region of low-energy nanoemulsions, electron paramagnetic resonance spectroscopy (EPR) with spin-probing was conducted. EPR is a non-destructive analytical technique and it is the only method available for the direct detection of paramagnetic species. In order to capture alterations in the interface of low-energy nanoemulsions in relation to their composition, 5-doxyl stearic acid (5-DSA, an amphiphilic molecule) was used for spin probing. In the presence of a surfactant membrane, 5-DSA aligns with the surfactant molecules, exposing the doxyl- group to the environment of the surfactant tails. Molecular motion of the 5-DSA reflects the properties of the interfacial microenvironment.

To obtain desired concentration of the spin probe in the nanoemulsions, 1 ml of each was added to a tube where the appropriate amount of the spin probe had been previously deposited (15μl of $7.8x10^{-3}$ M ethanolic stock solution of 5-DSA were transferred in the tube and the solvent was let to evaporate at room temperature). The samples were left overnight for incubation. The final concentration of 5-DSA in the samples was 0.117mM. Rotational correlation time (τ_R), as the most relevant parameter of the spin probe molecular motion, was calculated after spectral analysis.

EPR spectra were recorded using the Bruker EPR spectrometer (Billerica, USA), operating at the X-Band. The samples were inserted in the WG-813-Q Wilmad Suprasil flat cell (Buena, USA). Instrument settings were the following: center field - 0.349T; scan range - 0.01T; receiver gain – $5.64x10^3$; time constant – 5.12ms; modulation amplitude - 0.4mT; frequency - 9.78GHz. Data collecting and analysis were performed using the *BrukerWinEPR acquisition and processing* program. All spectral simulations were performed with home-written programs in MATLAB® (The MathWorks, Natick, USA) employing the *EasySpin toolbox* for EPR spectroscopy.

2.2.7. Density and viscosity measurements

Viscosity was measured using DV-I Prime viscometer (Brookfield Engineering Laboratories, USA), at a shear rate of 10 rpm, at 25 °C. For density evaluation, density meter DMA 4500 (Anton Paar GmbH, Austria) was used.

2.2.8. Antioxidant activity evaluation

Free radical scavenging activity of curcumin *per se* and from developed formulations was evaluated through DPPH (2, 2-diphenyl-1- picrylhydrazyl assay) assay using the protocol already described by Nikolic *et al*. For more details, please consult the *Supplementary material* section.

2.2.9. Release study of curcumin from the formulations

To determine the liberation profile of curcumin from developed formulations, *in vitro* release study was performed using Franz cells (n=6; Gauer Glas, D-Püttlingen, Germany), as already described in Nikolic et al (2018). As acceptor medium ethanol 50 % *v/v* was used (Nikolic et al, 2018). Each cell receptor chamber was filled with ethanol 50 % *v/v* (chamber volume: 12 mL; effective diffusion area: 2.01 cm^2), preheated to 32 ˚C. Polycarbonate membranes (Nuclepore™, Whatman, Maidstone, United Kingdom; pore diameter: 0.1 µm), activated in the same ethanol solution during the 12-hours period, were carefully placed on top of the receiver compartment,

and then the donor and acceptor chamber were fastened. Any existing air bubbles were removed. The donor chamber was filled with 1 g of the samples being investigated, and afterwards covered with silicone film (ParafilmTM, USA) to prevent evaporation and loss of the formulation during sampling. Cells were placed in the water bath where the temperature of 32 ˚C was maintained through the whole experiment. Acceptor phase was under continuous magnetic stirring at 500 rpm. Release study was performed for 6 hours. Aliquots of 0.6 µL of the acceptor phase were withdrawn at 6 time points (0.5 h, 1h, 2h, 3h, 4h and 6h), and then replaced with the same volume of fresh and thermostated ethanol solution. LC-MS/MS technique was used for determination of curcumin content. Aiming to find the model that best describes the drug liberation profile from investigated samples, cumulative amounts of curcumin per unit area were evaluated through several kinetic models.

2.2.10. *In vivo* evaluation of penetration of curcumin through superficial skin layers

To evaluate the penetration profile of curcumin through the skin from developed low-energy nanoemulsions, *in vivo* tape stripping was performed with four volunteers (female, aged 23-27, with no history of skin disease or hypersensitivity). The study was conducted in adherence to the Declaration of Helsinki. Local Ethical Committee of University of Belgrade – Faculty of Pharmacy had approved the study. After the potential volunteers had been informed about the study protocol and its aims in details, they provided written consent.

Three different formulations were tested, and 250 µl of each (a single application) was uniformly applied onto the previously marked sites (3x3 cm) on the inner, non-hairy regions of forearms. After 2 hours, 12 discoidal adhesive tapes (D-squame® tapes, CuDerm Corporation, USA, surface area 3.8 cm^2) were utilized for removal of stratum corneum layers at each treated place. Sampling sites were visibly marked to ensure site-precise tape removal. Each tape was placed on

the determined site, subjected to uniform pressure (140 g/cm^2) for 10 s, and then gently removed from the skin surface using precise tweezers. For the analysis of the amount of removed stratum corneum, gravimetric procedure was performed. Each adhesive tape was weighted on a high precision analytical balance (Sartorius BP210D, Goettingen, Germany), prior to and immediately after stripping. If the surface of the stripped area and the density of stratum corneum (1 g/cm^3) are known, then it is easy to convert the differential mass to the thickness of the removed stratum corneum layer with each tape, using the following equation:

$$\Delta m = P * x * \rho,$$

where Δm stands for the difference of the tape masses prior and after the treatment, P is stripping area (3.8 cm^2), x is the thickness of the removed stratum carenum area, and ρ is the density of stratum corneum (1 g/cm^3).

After the stripping, each tape was carefully transferred into a glass tube containing 4 mL of ethanol (50%, v/v). In order to extract curcumin, tubes were sonicated (Sonorex RK 120H, Bandelin, Berlin, Germany) for 15 min and afterwards centrifuged at 4000 rpm for 5 min (Centrifuge MPW-56; MPW Med. Instruments, Warszawa, Poland). Curcumin-containing supernatant was separated and immediately analyzed acquiring LC-MS/MS method. The total thickness of stratum corneum (L) was determined as described previously (Herkenne et al., 2007, Isailovic et al, 2016), through defined measurements of transepidermal water loss (prior to stripping, after 4th, 8th and 12th tape stripped) using Tewameter® TM 210 (Courage+Khazaka, Köln, Germany), precisely on the treated area. Consequently, the concentration profile of curcumin across the stratum corneum was expressed as a function of relative position (x/L), which enabled objective comparison of results obtained among different volunteers and different formulations.

2.2.11. Determination of curcumin concentration: LC-MS/MS technique

Accurate and precise determination of curcumin content in the formulations, as well as during drug release study, was performed by a liquid chromatography coupled with mass spectrometry (LC-MS/MS) technique. Liquid chromatographic system with Accela autosampler and the pump (Thermo Fisher Scientific, San Jose, CA) was applied, and analysis was conducted under established separation conditions. Xterra® MS C18 column (3,5µm 2,1x150mm; Waters Corporation, Ireland) was used for the separation, at 25 ºC. A mobile phase consisting of acetonitrile and 0.1% formic acid aqueous solution (70:30 v/v) was used for isocratic elution, at flow rate of 0.3 mL/min, and run time of 5 minutes. Mass analyses were conducted on TSQ Quantum Access MAX triple quadrupole mass analyzer equipped with electrospray ionization (ESI) source and high-purity nitrogen as nebulizing gas. Selected reaction monitoring (SRM) for data collecting was in positive mode, and ESI source and mass spectrometry parameters were at following values: spray voltage - 5000 V; vaporizer temperature - 400 ºC; sheath gas pressure - 30 units; ion sweep gas pressure - 0 units; auxiliary gas - 15 units; ion transfer capillary temperature - 250 ºC; capillary offset - 35 units; skimmer offset - 0 units; m/z 369,2→177,0; collision energy – 22 V; peak width - 0.7; scan time - 200 ms. The data were processed through Xcalibur software v 2.1.0.1139 (Thermo Fisher Scientific).

2.2.12. Statistical analysis

Whenever it was appropriate, results were presented as mean values ± SD. Relevant physicochemical parameters, as well as results of the *in vivo* measurements were assessed through a one-way ANOVA, followed by Tukey post hoc test.

3. RESULTS AND DISCUSSION

3.1.Physicochemical characterization

Based on the overall research work conducted by Nikolic et al (2018), F_MCT was selected as the starting formulation. In the formulations with monoterpenes, the only difference was in the composition of the oil phase – a part of MCT was replaced by eucalyptol or pinene. Qualitative and quantitative composition of all investigated formulations is given in the Table 1.

Each formulation was first visually observed and then subjected to further analysis. All nanoemulsions were easily flowable, with bluish reflection. Interestingly, the droplet size decreased (Table 2) and the nanoemulsions' transparency increased significantly when part of the MCT was replaced by the terpenes in both blank and curcumin-loaded nanoemulsions. Such observation might indicate potential physical interaction and rearrangements in the interfacial area of the low-energy nanoemulsions.

In order to check this assumption, EPR spectroscopy was performed with blank low-energy nanoemulsions, with the idea to have an insight into the dynamics of their interfacial area. Due to the amphiphilic nature of the 5-DSA, when mixed with a nanoemulsion, it localizes at the water/oil interface. As a result, any dynamic alteration in the interfacial layer caused by the presence of specific molecules may be captured. (Mitsou et al, 2018; Klare and Steinhoff, 2009; Berliner and Rauben, 2012).

For each blank nanoemulsions, obtained rotational correlation time values (τ_R, Table 3, Figure 1) indicated the presence of two different microenvironments for the 5-DSA: one where 5-DSA is strongly immobilized (higher τ_R), and a more flexible one (lower τ_R). Since two structurally different surfactants were used in combination (polysorbate 80 and soybean lecithin, in the ratio 9:1) to provide efficient stability to the nanoemulsion, these two microenvironments could be linked to the surfactant distribution. Some of the spin probe molecules were located in between molecules of only polysorbate 80 molecules (more flexible microenvironment – microenvironment 1) and others were in the regions where both surfactants were present (more rigid microenvironment – microenvironment 2). Probably, lecithin, having the structure more complex than polysorbate 80, makes the interfacial motion more difficult (Avramiotis et al, 2000).

Nevertheless, it should be emphasized that both populations (so-called "slow" and "fast") belong to the region of slow motion (telling that the 5-DSA microenvironment is very strict in each case), but these terms are used for the ease of understanding and differing.

Another important parameter obtained from the EPR spectral analysis is the isotropic hyperfine splitting constant ($\alpha'o$), which is sensitive to the micropolarity of the environment close to the paramagnetic ring of the probe. It increases when the polarity of the area near the spin probe is increased (Papadimitriou et al, 2008). In the present study, $\alpha'o$ values (Table 3) are higher when the spin probe molecule is located in the microenvironment 2. Assuming that the complex structure of the lecithin molecule creates a hurdle for the amphiphilic spin probe to enter deeper in the surfactant layer (Avramiotis et al, 2000), 5-DSA becomes more exposed to the polar, continuous phase.

After the introduction of eucalyptol and pinene in the oil phase, τR values have been changed for both microenvironments. Perhaps the rearrangement in the interfacial packing was caused by the presence of more molecular species at the interface, thus reflecting the motion of the 5-DSA. Consequently, it may be suggesting that eucalyptol and pinene participate in the interfacial layer. If we link this finding to their effect on droplet size, it can be assumed that eucalyptol and pinene express surfactant-like activity (costabilizing effect), influencing the surfactant curvature at the interface of low-energy nanoemulsions. Similar was observed for eucalyptol by Zänker et *al* (1980), after the tensiometry experiments. In order to be sure about the exact site of the observed alteration, pH of the formulations should be considered. pKa of the 5-DSA is 6.55, meaning that in the tested formulations, 5-DSA is dominantly in the unionized form. Accordingly, the main locus for 5-DSA is closer to the nonpolar region of the interfacial layer.

It is known that the viscosity and the density of the oil phase can influence the process of nanoemulsification, which is especially important in the low-energy processes (Tadros *et al*, 2004) Therefore, viscosity of the oil phase, surfactant-oil blends and low-energy nanoemulsions was assessed (Table 5). As expected, MCT has a higher viscosity compared to the terpene compounds. Consequently, oil mixtures have lower viscosity than the MCT, which can also cause the droplet size to decrease. However, the viscosity of each nanoemulsions is very close, regardless the oil phase composition, suggesting that this difference does not influence the final formulation properties.

Furthermore, in order to give the final argument in favor of the statements about the co-stabilizing phenomenon attributed to the investigated terpene compounds, formulations with the same oil content and composition were prepared but varying only the *surfactant-to-oil ratio* (SOR). Interestingly, for terpene-containing nanoemulsions the lowest SOR able to give stable

nanoemulsions was 0.3 (Table 6), whereas, as already reported by Nikolic *et al* (2018), in the case of the nanoemulsions containing only MCT as the oil phase, SOR below 0.75 did not meet the nanoemulsions formation. This decrease in droplet size with higher SOR follows the 2nd polynomial regression (Figure 2A). The functions describing this trend are negative in the whole tested are for both terpene-containing formulations. The first derivative calculations pointed out that with a small increase in surfactant concentration the extent of the droplet diameter reduction is intense, especially until the SOR 0.5. After this value, the change is less significant (Figure 2B). This statement can also be supported if the data on effective alkane carbon number (EACN) are taken into consideration. Namely. the EACN values are telling about the "oiliness" of the oil – the higher hydrophobicity of the oil, the higher EACN value. Literature suggests that the EACN of medium-chain triglyceride oils is around 16, pinene has EACN 3.6, and eucalyptol can also be characterized as relatively polar oil as it is cyclic compound with oxygen in the structure (Bouton et al, 2009; Engelskirchen et al, 2007; Acosta et al, 2003). This "polar" nature of these terpene oils enables the interactions with surfactants and easier solubilization process, which is in line with the idea of their surface-activity, and co-stabilizing properties.

Finally, visualization of the dispersed nanodroplets was performed through atomic force microscopy (Figure 3). Contrastingly, compared to the morphological properties of the F_MCT, which were previously analyzed (Nikolic *et al*, 2018), here the droplets are regular spheres, and it is visible that the droplets much smaller than 100 nm are dominant. This regular shape gives rise to the conclusion that these terpene compounds probably influence the interfacial curvature, affecting the monolayer morphology. What is more, topography analysis showed that the droplet surface is smooth and regular, which was not the case with the formulation F1_MCT, where droplets were of irregular shape and bumpy.

3.2.Curcumin encapsulation, antioxidant evaluation of the formulations and release kinetics

In order to ensure the good and reliable comparison among formulations, the ones with SOR 1 were chosen for curcumin encapsulation, and their properties were checked, focusing on the performance of curcumin within the formulations. Droplet size followed the same trend as in the blank formulations (Table 2), and pH was in accordance with the stability requirements for curcumin (Sharma *et al*, 2005).

Encapsulation of curcumin affected microstructural organization, implying that some interactions occur at the interface (Table 4). Curcumin's encapsulation induced an increase in the τ_R for the "more flexible" microenvirnonment while in the same parameter of the "more rigid" microenvironment decreased. Such finding could be due to the curcumin's interactions with the hydrophobic chains of the surfactant layer.

To check the antioxidant activity after encapsulation, DPPH assay was performed. Even though it is known that curcumin possesses remarkable antioxidant activity (Nikolic et al, 2018), this experiment was performed with the view to check whether the emulsification process or any interaction during formulation preparation would influence its stability and activity. Based on obtained results, curcumin exhibited high scavenging activity, regardless of the formulation type (Figure 4). The pH values of each formulation supported the high proton-donating ability of curcumin, enabling it to neutralize the free radical. Calculated IC_{50} value was in accordance with already reported results - 0.11 mg/ml (Nikolic *et al*, 2018). These results suggested that no alterations in antioxidant power occurred after curcumin's encapsulation in terpene-containing low-energy nanoemulsions.

Knowing that for the *in vivo* effects the appropriate release of the active ingredient from the formulation is a prerequisite, liberation profiles of curcumin were evaluated using *Franz* diffusion cells. Performed experiments indicated that release profile from eucalyptol- and pinene-loaded nanoemulsions followed Higuchi kinetics, which was the case with the F_MCT, as well (Figure 6). The difference between terpene-containing formulations and the terpene-free one can be noticed – F_EUC and F_PIN exhibit higher release (14.0±0.2% and 13.9±0.1%, respectively) compared to F_MCT (10.1±0.2) after 6 hours of the experiment. ~~In addition, as it is visible from the Figure 6~~, The difference is more intense starting from the 3rd hour.

Attempting to correlated microstructural characterization (EPR study) with the release kinetics, an interesting finding was made. Namely, observed changes in the surfactant monolayer flexibility upon curcumin encapsulation did not significantly affect the release kinetics. More precisely, in order to describe the effective frictional forces that the probe molecule experiences under rotation at the interfacial layer, microviscosity could be analyzed. Consequently, the same parameter can be used to characterize the environment to which an active molecule is exposed prior to the release (Mikosh et al, 1994). Based on the EPR measurements of the rotational correlation time, the viscosity of the environment of a spin probe (microviscosity) may be estimated utilizing the Debye-Stokes-Einstein equation (Bales and Zana, 2002; Berliner and Rauben1, 2012):

$$\tau R = 4/3R\hat{}3\pi\eta KT \qquad (1);$$

where η is the shear viscosity of the solvent, K the Boltzmann constant, T the absolute temperature, and R the hydrodynamic radius of the molecule.

Clearly, as microviscosity increase, τR also increase. Such observation may be used in order to link the release rate (diffusion) of the active molecule to the microstructural studies. Accordingly, for higher microviscosity, lower diffusivity would be expected. However, in the present study, no such correlation was observed. In the *in vitro* release study, formulation with monoterpene compound presented higher release compared to the formulation containing only MCT as the oil phase, which would not be expected after the microstructural study (Tables 3 and 4), because these formulations exhibited higher τR values. It appears that the flexibility of the interfacial layer is not crucial for the release of curcumin. Similar was observed by Kalaitzaki et al (2014). However, it is known that the main driving force for diffusion across the membrane is the thermodynamic activity of the active molecule in the formulation, which is reflected by its initial concentration and saturation solubility in the formulation and acceptor compartment (Karsa and Stephenson, 1996). As these low-energy nanoemulsions did not differ significantly in the bulk viscosity, and structural investigation did not correlate with the obtained data, the only explanation for such finding could be that the presence of volatile terpene compounds (after 2-3 hours, due to some evaporation) induced the decrease in the saturation solubility of curcumin in the formulations, encouraging the escaping tendency of the molecule from the nanoemulsions (Karsa and Stephenson, 1996).

3.3.In vivo penetration evaluation

The extent of curcumin delivery into the *stratum corneum* was significantly higher for F_EUC (34.24±5.68 μg/cm^2), compared to other two formulations (30.62±2.61 μg/cm^2 for F_MCT and 21.61±4.01 μg/cm^2 for F_PIN) (Figure 6). Even though it was expected that both terpenes would give a pronounced effect, pinene did not meet the imposed expectations - it had the lowest performance~~, which was even more surprising.~~ This was the case where *in vivo* significant

difference in penetration did not match the results after the *in vitro* release experiments. Similar findings were already reported for other model active substances (Jaksic *et al*, 2012). As there is no viscosity difference among the formulations (Table 5), and similar microstructural behavior was described through the EPR measurements, it seems reasonable to conclude that ~~expressed difference may be due to the different~~ solubility of curcumin in the oil phases used for preparation of these low-energy nanoemulsions governed the penetration through the superficial skin layers. Namely, saturation solubility of curcumin follows the *in vivo* skin penetration results: solubility is the highest in eucalyptol (4.18±0.02 mg/ml), then in MCT (1.67 ± 0.04 mg/ml) and then in pinene (0.21±0.01 mg/ml). Probably, penetration of eucalyptol in the tissue alters the solubility properties of the superficial skin layers. It modifies the thermodynamic activity of the drug, and upon evaporation, it provides a supersaturated state which promotes penetration, supporting the escape of curcumin from the nanoemulsion droplets (Parhi and Swain, 2018). In the case of MCT, there was no evaporation of the oil. However, curcumin has much higher solubility in the MCT than in pinene, it seems logical that MCT, due to higher solubility, enabled better diffusion of curcumin through the skin.

Additionally, there may exist some cross activity of the enhancers (lecithin and polysorbate 80 are also declared as penetration enhancers (Lane, 2013)), so the diffusion through the skin and penetration extent could not be always so easily explained only by concentration gradient.

4. CONCLUSION

In this study, the idea was to link microstructural properties to biopharmaceutical performances of monoterpene low-energy nanoemulsions for improved dermal delivery of curcumin. Evaluating the potential of monoterpene compounds eucalyptol and pinene to deliver curcumin into the *stratum corneum*, it was demonstrated that the solubility of the active molecule within the oil phase is a key feature for delivery into the skin, regardless of the penetration enhancement mechanism that stands in behind. Moreover, in attempting to correlate the data obtained through several complementary techniques, it was highlighted that physicochemical characterization methods cannot be independently used to predict the biopharmaceutical performances and the *in vivo* fate of an active molecule.

In addition, during the microstructural study, it was proved that that monoterpene compounds eucalyptol and pinene strongly modify the nanoemulsion interfacial environment. They reduced the amount of surfactant needed for obtaining stable

formulations with significantly smaller droplet size. Observed additional terpenes' role overcomes their already established penetration enhancement effect. Such properties should be further exploited with the view to obtain topical formulation with enhanced penetration efficacy, and better safety profile due to lower surfactant content.

5. CONFLICT OF INTEREST

The authors have no financial or non-financial interests that represent potential conflict of interests.

6. ACKNOWLEDGEMENT

The authors are grateful to the Ministry of Education, Science and Technological Development of the Republic of Serbia, for supporting this research within the framework of the project TR34031 *Development of Micro- and Nanosystems as Carriers for Drugs with Anti-inflammatory Effect and Methods for Their Characterization*, as well as through the project TR32008 *Micro- and Nanosystems for Power Engineering, Process Industry and Environmental Protection.* This work was also supported by the bilateral project between the Republic of Serbia and the Federal Republic of Germany *Biosurfactants and biopolysaccharides/film-forming polymers as cosmetic raw materials and prospective pharmaceutical excipients: formulation of colloidal and film-forming delivery systems.*

7. REFERENCES

1. Acosta, E., Szekeres, E., Sabatini, D. A., & Harwell, J. H., 2003. Net-average curvature model for solubilization and supersolubilization in surfactant microemulsions. Langmuir. *19*(1), 186-195. https://doi.org/10.1021/la026168a.
2. Ahad, A., Aqil, M., Kohli, K., Chaudhary, H., Sultana, Y., Mujeeb, M., Talegaonkar, S. 2009. Chemical penetration enhancers: a patent review. *Expet Opin Ther Pat. 19*(7), 969-988. https://doi.org/10.1517/13543770902989983.
3. Ahangari, N., Kargozar, S., Ghayour- Mobarhan, M., Baino, F., Pasdar, A., Sahebkar, A., Ferns, G.A.A., Kim, H.W., Mozafari, M., 2019. Curcumin in tissue engineering: A traditional remedy for modern medicine. Biofactors. *45*(2), 135-151. https://doi.org/10.1002/biof.1474.
4. Avramiotis, S., Cazianis, C. T., & Xenakis, A. (2000). Membrane spin-probe studies in lecithin and bis (2-ethylhexyl) sulfosuccinate sodium salt water-in-oil microemulsions.

In *Trends in Colloid and Interface Science XIV* (pp. 196-200). Springer, Berlin, Heidelberg. https://doi.org/10.1007/3-540-46545-6_40

5. Berliner, L. J., Reuben, J. (Eds.), 2012. *Spin labeling: theory and applications* (Vol. 8). Springer, Berlin.
6. Bilia, A. R., Guccione, C., Isacchi, B., Righeschi, C., Firenzuoli, F., Bergonzi, M. C., 2014. Essential oils loaded in nanosystems: a developing strategy for a successful therapeutic approach. Evid. Based Complement. Alternat. Med. https://doi.org/10.1155/2014/651593.
7. Bouton, F., Durand, M., Nardello-Rataj, V., Serry, M., Aubry, J. M., 2009. Classification of terpene oils using the fish diagrams and the Equivalent Alkane Carbon (EACN) scale. Colloid. Surface. A. *338*(1-3), 142-147. https://doi.org/10.1016/j.colsurfa.2017.07.068.
8. Chen, J., Jiang, Q.D., Chai Y.P., Zhang, H., 2016. Natural Terpenes as Penetration Enhancers for Transdermal Drug Delivery. Molecules, *21*(12), 1709. https://doi.org/10.3390/molecules21121709.
9. Choudhary, V., Shivakumar, H., Ojha, H., 2019. Curcumin-loaded liposomes for wound healing: Preparation, optimization, in-vivo skin permeation and bioevaluation. J. Drug. Deliv. Sci. Tec. *49*, 683-691. https://doi.org/10.1016/j.jddst.2018.12.008.
10. De Matos, S. P., Teixeira, H. F., de Lima, Á. A., Veiga-Junior, V. F., Koester, L. S., 2019. Essential Oils and Isolated Terpenes in Nanosystems Designed for Topical Administration: A Review. *Biomolecules*, *9*(4), 138. https://doi.org/10.3390/biom9040138

11. Dos Anjos, J. L. V., de Sousa Neto, D., Alonso, A., 2007. Effects of 1, 8-cineole on the dynamics of lipids and proteins of stratum corneum. Int. J. Pharm. *345*(1-2), 81-87. https://doi.org/10.1016/j.ijpharm.2007.05.041.
12. Engelskirchen, S., Elsner, N., Sottmann, T., Strey, R., 2007. Triacylglycerol microemulsions stabilized by alkyl ethoxylate surfactants—a basic study: phase behavior, interfacial tension and microstructure. J. Colloid. Interf. Sci. *312*(1), 114-121. https://doi.org/10.1016/j.jcis.2006.09.022.
13. Haque, T., Talukder, M. M. U. (2018). Chemical Enhancer: A Simplistic Way to Modulate Barrier Function of the Stratum Corneum. Adv. Pharm. Bull. *8*(2), 169-179. https://doi.org/10.15171/apb.2018.021.
14. Herkenne, C., Naik, A., Kalia, Y. N., Hadgraft, J., Guy, R. H., 2007. Dermatopharmacokinetic prediction of topical drug bioavailability in vivo. J. Invest. Dermatol. *127*(4), 887-894. https://doi.org/10.1038/sj.jid.5700642.
15. Isailović, T., Đorđević, S., Marković, B., Ranđelović, D., Cekić, N., Lukić, M., Pantelic, I., Daniels, R., Savić, S., 2016. Biocompatible nanoemulsions for improved aceclofenac skin delivery: formulation approach using combined mixture-process experimental design. *J. Pharm. Sci. 105*(1), 308-323. http://doi.org/10.1002/jps.24706.
16. Jaksic, I., Lukic, M., Malenovic, A., Reichl, S., Hoffmann, C., Müller-Goymann, C., Daniels, R., Savic, S., 2012. Compounding of a topical drug with prospective natural surfactant-stabilized pharmaceutical bases: physicochemical and in vitro/in vivo characterization–a ketoprofen case study. Eur. J. Pharm. Biopharm. *80*(1), 164-175. http://doi.org/10.1016/j.ejpb.2011.09.001.

17. Karande, P., Mitragotri, S., 2009. Enhancement of transdermal drug delivery via synergistic action of chemicals. *BBA-Biomembranes*. *1788*(11), 2362-2373. https://doi.org/10.1016/j.bbamem.2009.08.015.

18. Karsa, D. R., Stephenson, R. A. (Eds.)., 1996. *Chemical aspects of drug delivery systems* (Vol. 178). Royal Society of Chemistry, London.

19. Kalaitzaki, A., Poulopoulou, M., Xenakis, A., Papadimitriou, V., 2014. Surfactant-rich biocompatible microemulsions as effective carriers of methylxanthine drugs. *Colloid Surface A. 442*, 80-87. https://doi.org/10.1016/j.colsurfa.2013.05.055

20. Klare, J. P., Steinhoff, H. J., 2009. Spin labeling EPR. Photosynth. Res. *102*(2-3), 377-390. http://doi.org/10.1007/s11120-009-9490-7.

21. Komaiko, J. S., McClements, D. J., 2016. Formation of food- grade nanoemulsions using low- energy preparation methods: A review of available methods. Compr. Rev. Food Sci. F. *15*(2), 331-352. https://doi.org/10.1111/1541-4337.12189.

22. Krukiewicz, K., Zak, J. K., 2016. Biomaterial-based regional chemotherapy: local anticancer drug delivery to enhance chemotherapy and minimize its side-effects. Mater. Sci. Eng. C Mater. Biol. Appl. *62*, 927-942. https://doi.org/10.1016/j.msec.2016.01.063.

23. Lane, M. E., 2013. Skin penetration enhancers. Int. J. Pharm. *447*(1-2), 12-21. https://doi.org/10.1016/j.ijpharm.2013.02.040.

24. Mason, T. G., Wilking, J. N., Meleson, K., Chang, C. B., Graves, S. M., 2006. Nanoemulsions: formation, structure, and physical properties. *J Psys Condens Matter*. *18*(41), R635. https://doi.org/10.1088/0953-8984/18/41/R01

25. Mikosch, W., Dorfmüller, T., Eimer, W., 1994. Rotational diffusion in polyacrylamide gels as a function of solvent quality. *J Chem Phys. 101*(12), 11052-11059. https://doi.org/10.1063/1.468480

26. Mishra, H., Mishra, P. K., Ekielski, A., Jaggi, M., Iqbal, Z., Talegaonkar, S., 2018. Melanoma treatment: From conventional to nanotechnology. J. Cancer. Res. Clin. *144*(12), 2283-2302. https://doi.org/10.1007/s00432-018-2726-1.

27. Mitsou, E., Kalogianni, E. P., Georgiou, D., Stamatis, H., Xenakis, A., Zoumpanioti, M., 2018. Formulation and structural study of a biocompatible water-in-oil microemulsion as an appropriate enzyme carrier: The model case of Horseradish peroxidase. *Langmuir*, *35*(1), 150-160. https://doi.org/10.1021/acs.langmuir.8b03124.

28. Mohammed, D., Hirata, K., Hadgraft, J., Lane, M. E., 2014. Influence of skin penetration enhancers on skin barrier function and skin protease activity. Eur. J. Pharm. Sci. *51*, 118-122. https://doi.org/10.1016/j.ejps.2013.09.009.

29. Mouthuy, P. A., Škoc, M. S., Gašparović, A. Č., Milković, L., Carr, A. J., Žarković, N., 2017. Investigating the use of curcumin-loaded electrospun filaments for soft tissue repair applications. Int. J. Nanomedicine. *12*, 3977. https://doi.org/10.2147/IJN.S133326.

30. Münch, S., Wohlrab, J., Neubert, R. H. H., 2017. Dermal and transdermal delivery of pharmaceutically relevant macromolecules. *Eur Jour Pharm Biopharm. 119*, 235-242. https://doi.org/10.1016/j.ejpb.2017.06.019.

31. Nabavi, S. M., Russo, G. L., Tedesco, I., Daglia, M., Orhan, I. E., Nabavi, S. F., Bishayee, A., Nagulapalli Venkata K., Abdollahi M., Hajheydari, Z., 2018. Curcumin and melanoma: from chemistry to medicine. Nutr. Cancer. *70*(2), 164-175. https://doi.org/10.1080/01635581.2018.1412485.

32. Neubert, R. H., 2011. Potentials of new nanocarriers for dermal and transdermal drug delivery. Eur J Pharm Biopharm. *77* (1), 1-2. https://doi.org/10.1016/j.ejpb.2010.11.003.

33. Nikolic, I., Lunter, D. J., Randjelovic, D., Zugic, A., Tadic, V., Markovic, B., Cekic, N., Zivkovic, L., Topalovic, D., Potparevic, B., Daniels, R., Savic, S., 2018. Curcumin-loaded low-energy nanoemulsions as a prototype of multifunctional vehicles for different administration routes: Physicochemical and in vitro peculiarities important for dermal application. Int. J. Pharm. *550*(1-2), 333-346. https://doi.org/10.1016/j.ijpharm.2018.08.060.

34. Panahi, Y., Fazlolahzadeh, O., Atkin, S. L., Majeed, M., Butler, A. E., Johnston, T. P., Sahebkar, A., 2019. Evidence of curcumin and curcumin analogue effects in skin diseases: A narrative review. J. Cell. Physiol. *234*(2), 1165-1178. https://doi.org/10.1002/jcp.27096.

35. Papadimitriou, V., Pispas, S., Syriou, S., Pournara, A., Zoumpanioti, M., Sotiroudis, T. G., Xenakis, A., 2008. Biocompatible microemulsions based on limonene: formulation, structure, and applications. *Langmuir*, *24*(7), 3380-3386. https://doi.org/10.1021/la703682c.

36. Parhi, R., Swain, S., 2018. Transdermal Evaporation Drug Delivery System: Concept to Commercial Products. Adv. Pharm. Bull. *8*(4), 535. https://doi.org/0.15171/apb.2018.063.

37. Pham, Q. D., Topgaard, D., Sparr, E., 2015). Cyclic and linear monoterpenes in phospholipid membranes: phase behavior, bilayer structure, and molecular

dynamics. *Langmuir*, *31*(40), 11067-11077. https://doi.org/10.1021/acs.langmuir.5b00856

38. Sharma, R. A., Gescher, A. J., Steward, W. P., 2005. Curcumin: the story so far. *Eur J Cancer*, *41*(13), 1955-1968. https://doi.org/10.1016/j.ejca.2005.05.009
39. Tadros, T., Izquierdo, P., Esquena, J. and Solans, C., 2004. Formation and stability of nano-emulsions. *Adv Colloid Interface Sci*, *108*, pp. 303-318. https://doi.org/10.1016/j.cis.2003.10.023
40. Thangapazham R.L., Sharma A., Maheshwari R.K. (2007) Benefitial role of curcumin in skin diseases. In: Aggarwal B.B., Surh YJ., Shishodia S. (eds) The Molecular Targets and Therapeutic Uses of Curcumin in Health and Disease. Advances in experimental medicine and biology, Vol. 595. Springer, Boston, MA
41. Ud Din, F., Aman, W., Ullah, I., Qureshi, O. S., Mustapha, O., Shafique, S., Zeb, A., 2017.Effective use of nanocarriers as drug delivery systems for the treatment of selected tumors. *IInt J Nanomed. 12*, 7291. https://doi.org/10.2147/IJN.S146315
42. Vaughn, A. R., Branum, A., Sivamani, R. K., 2016. Effects of turmeric (Curcuma longa) on skin health: A systematic review of the clinical evidence. Phytother. Res. *30*(8), 1243-1264. https://doi.org/10.1002/ptr.5640.
43. Yang, R., Wei, T., Goldberg, H., Wang, W., Cullion, K., & Kohane, D. S., 2017. Getting drugs across biological barriers. *Adv Mater*. *29*(37), 1606596. https://doi.org/10.1002/adma.201606596
44. Zänker, S., Tölle, W., Blümel, G., Probst, J., 1980. Evaluation of surfactant-like effects of commonly used remedies for colds. Respiration. *39*(3), 150-157. https://doi.org/10.1159/000194210.

45. Zsikó, S., Csányi, E., Kovács, A., Budai-Szűcs, M., Gácsi, A., Berkó, S., 2019. Methods to Evaluate Skin Penetration In Vitro. *Sci Pharm*. *87*(3), 19. https://doi.org/10.3390/scipharm87030019

46. Zhu, X. M., Li, Y., Xu, F., Gu, W., Yan, G. J., Dong, J., Chen, J., 2019. Skin Electrical Resistance Measurement of Oxygen-Containing Terpenes as Penetration Enhancers: Role of Stratum Corneum Lipids. Molecules. *24*(3), 523. https://doi.org/10.3390/molecules24030523.

FIGURE CAPTIONS

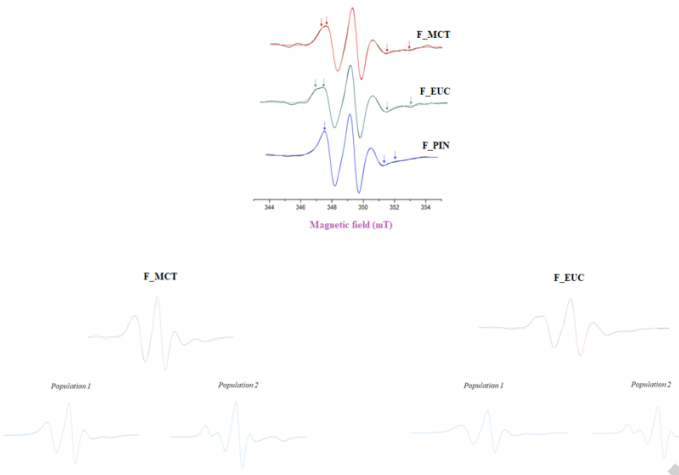

Figure 1. EPR spectra of the low-energy nanoemulsions: blank formulations

Results represent the mean value of 3 independent replications.

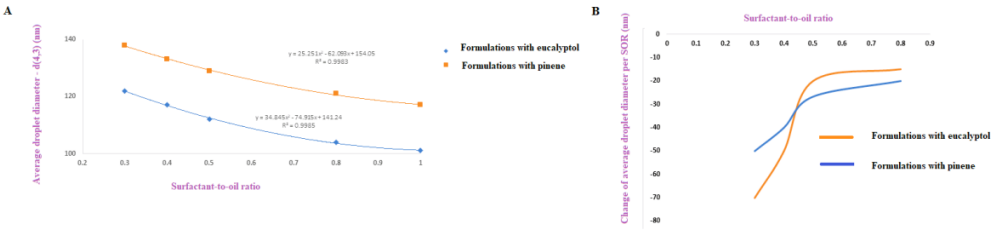

Figure 2. A: Change of the average droplet diameter with an increase in the surfactant-to-oil ratio (described through the 2nd polynomial regression); B: First derivative of the function

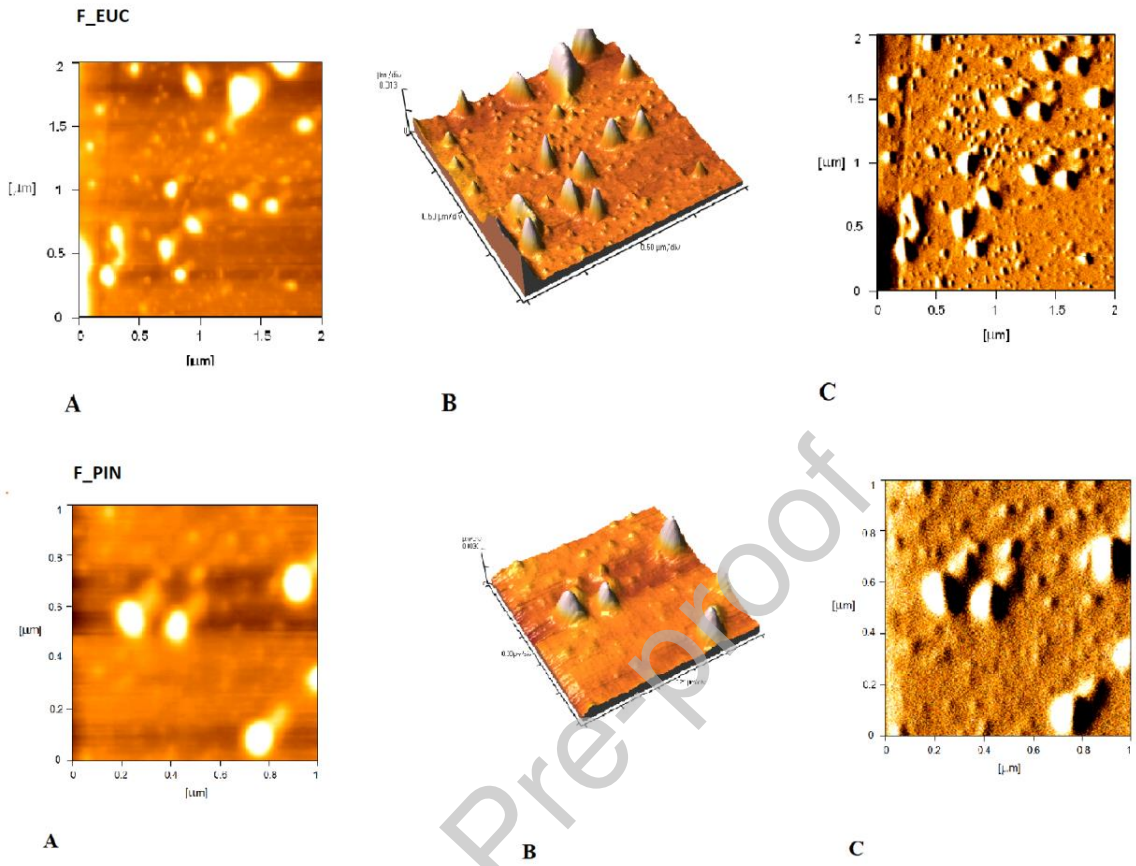

Figure 3. AFM micrographs of the terpene-containing low-energy nanoemulsions; A: 2D images, B: 3D images, C: signal-error images

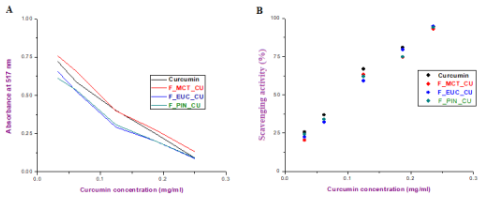

Figure 4. DPPH antioxidant evaluation of free curcumin and curcumin-loaded low-energy nanoemulsions; A: DPPH absorbance dependence on curcumin concentration, B: Percentage of antioxidant activity for different concentrations of curcumin

Results represent the mean value of 3 independent replications. There is no statistically significant difference among the antioxidant activity of the tested samples.

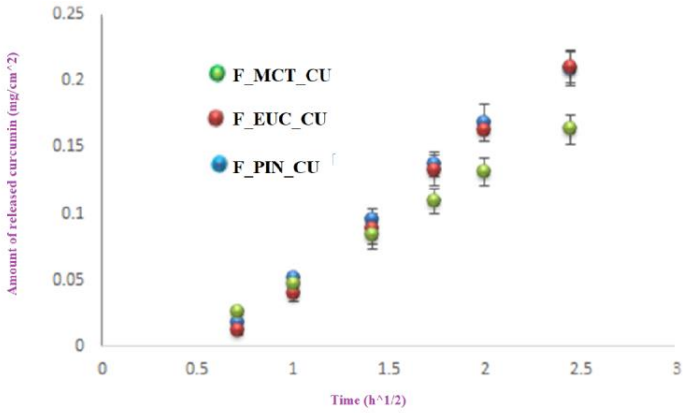

Figure 5. Release kinetics determination of curcumin-loaded low-energy nanoemulsions

Results represent the mean value of 6 independent replications ± standard deviation.

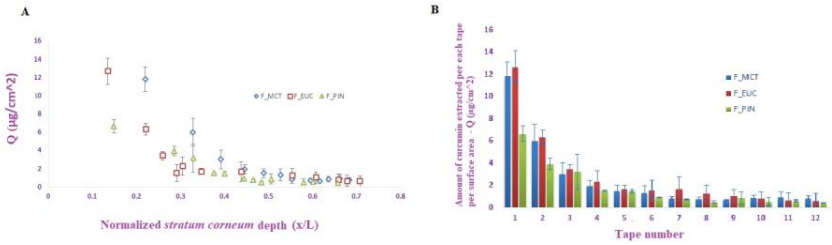

Figure 6. Analysis of curcumin penetration through the *stratum corneum*, A: Penetration profile of curcumin from different formulations, B: Amount of curcumin extracted per each tape;

Presented data are the result of 4 independent replications ± standard deviation.

F_PIN exhibited statistically lower penetration of curcumin ($p<0.05$) through the *stratum corneum* compared to F_EUC and F_PIN

Table 1. Concentration (%) of each component in the tested formulations

Formulation	MCT	Eucalyptol	Pinene	Curcumin	Soybean lecithin	Polysorbate 80	Ultrapure water
F_MCT	10	/	/	/	1	9	80
F_EUC	5	5	/				
F_PIN	5	/	5				
F_MCT_CU	10	/	/	0.3			79.7
F_EUC_CU	5	5	/				
F_PIN_CU	5	/	5				

Table 2. Results of the sizing analysis, pH and electrical conductivity

Formulation	d(10) (nm)	d(50) (nm)	d(90) (nm)	d[4, 3] (nm)	pH	Electrical conductivity (µS/cm)
F_MCT	81	125	197	132	4.78±0.05	97.1±5.1
F_EUC	79	95	128	101*	6.25±0.1	104.7±0.3
F_PIN	74	105	138	117*	4.65±0.1	100.3±0.7
F_MCT_CU	63	119	206	128	5.6±0.1	95.1±0.9
F_EUC_CU	65	93	127	102#	6.4±0.05	99.7±1.5
F_PIN_CU	69	109	135	115#	4.5±0.1	96.5±1.1

*p<0.05 compared to F_MCT
#p<0.05 compared to the F_MCT_CU
Presented data are the mean values of 3 independent replications

Table 3. Hyperfine splitting constant (α′o), rotational correlation time (τR) values and volume distribution of the spin probe in two different microenvironments

Formulation	$\alpha'o_1$	τ_{R1} (ns)	Volume distribution of the microenvironment 1 (%)	τ_{R2} (ns)	$\alpha'o_2$	Volume distribution of the microenvironment 2 (%)
F_MCT	13.30±0.07	4.9±0.2	87.4±2.1	12.8±0.4	14.93±0.16	12.6±2.7
F_EUC	13.35±0.19	5.7±0.3	88.6±2.4	14.4±0.3	14.77±0.37	11.4±2.4
F_PIN	13.42±0.06	4.3±0.5	87.9±2.1	13.8±0.3	14.61±0.07	12.1±1.90

Presented data are the mean values of 3 independent replications ± standard deviation.

Table 4. Rotational correlation time (τ_R) of the spin probe in two different microenvironments in the curcumin-loaded formulation

Formulation	τ_{R1} (ns)	τ_{R2} (ns)
F_MCT_CU	5.5±0.2	6.5±0.1
F_EUC_CU	8.5±0.2	13.4±0.5
F_PIN_CU	5.9±0.4	13.2±0.2

Presented data are the mean values of 3 independent replications ± standard deviation

Table 5. Viscosity and density results for the different oils used for the preparation of the nanoemulsions

Oil type	Viscosity (cP)	Density (g/cm^3)
MCT	23.58±0.19	0.94289±0.00010
EUC	2.58±0.01	0.92229±0.00008
PIN	1.32±0.01	0.85674±0.00031
EUC/MCT (1:1)	3.34±0.14	0.93150±0.00014
PIN/MCT (1:1)	2.3±0.11	0.90007±0.00007

Presented data are the mean values of 3 independent replications ± standard deviation

Table 6. Sizing results of the low-energy nanoemulsions prepared with different surfactant-to-oil rations

Formulation	**d(10) (nm)**	**d(50) (nm)**	**d(90) (nm)**	**d[4, 3] (nm)**
SOR 0.8_MCT/EUC	69	102	139	104
SOR 0.5_MCT/EUC	72	105	156	111
SOR 0.4_MCT/EUC	71	110	160	117
SOR 0.3_MCT/EUC	78	116	174	122
SOR 0.8_MCT/PIN	67	118	145	121
SOR 0.5_MCT/PIN	69	123	153	128
SOR 0.4_MCT/PIN	73	129	167	133
SOR 0.3_MCT_PIN	72	132	173	138

SOR – surfactant-to-oil ratio
Presented data are the mean values of 3 independent replications.

Graphical Abstract